scientific reports

OPEN

In vitro cytotoxicity evaluation of green synthesized alumina nanoscales on different mammalian cell lines

Alhaji Modu Bukar[1,2,5✉], Faez Firdaus Abdullah Jesse[3], Che Azurahanim Che Abdullah[4,5,6], Mustapha M. Noordin[1], Modu Z. Kyari[2], Ashreen Norman[4] & Mohd Azmi Mohd-Lila[1✉]

Nanoscale research is gaining interest in the biomedical, engineering, and environmental fields. Current expensive traditional chemical methods for synthesizing nanoparticles (NPs) inevitably lead to the synthesis of NPs with potentially less or no toxic effects on living cells. To overcome these challenges, in this study, we use a simple, inexpensive, and less toxic one-pot green chemistry approach instead of a chemical method to synthesize alumina nanoparticles (AlNPs) from *Carica papaya* extract. Nano-alumina has been widely studied due to its remarkable biological and physiochemical properties at nanoscale. However, to date, its biomedical application is limited due to the lack of sufficient data on cytotoxicity in living cells. The physicochemical properties of nano-alumina were determined by FT-IR, DLS, SEM and HRTEM. The cytotoxic effects of the synthesized nano-alumina were studied in cell lines LT and VERO at concentrations of 10–480 µg/mL in vitro. The cell viability of nano-alumina was evaluated using the MTT assay and the AO /EB double staining technique. Our results based on DLS and HRTEM analyzes confirmed spherical AlNPs with a zeta potential and average particle size of – 25 to 5 mV and 52 nm, respectively. The nano-alumina tested showed low toxicity to both cell lines after 28- and 48-h exposure. Furthermore, cell viability statistically decreased with increasing incubation time and concentration of AlNPs up to 480 µg/mL ($p < 0.001$). However, a minimal increase in cytotoxicity was observed at threshold levels in the range of 120–480 µg/mL. The half-maximal inhibitory concentration (IC_{50}) of AlNPs in the VERO and LT cell lines were 153.3, 252.0 µg/mL and 186.6, 395.3 µg/mL, respectively, after 24- and 48-h exposure to AlNPs. Thus, we conclude that the cytotoxic effect of AlNPs depends on the concentration, exposure time and cell type. The result suggests that the concentration used in this study may be useful for biomedical applications.

Nanoscale research has been widely studied due to their remarkable biological and physiochemical properties. Nanoparticles are organic or inorganic particles ranging in size from 1 to 100 nm. Organic nanoparticles such as immunostimulatory complexes (ISCOMs), lipid-based, polymer-based, virus-like, and nanoemulsions are relatively biocompatible, biodegradable, and less toxic[1,2]. On the other hand, inorganic nanoparticles synthesized from metal oxides such as aluminum oxide, zinc oxide[3,4], and silver oxide are relatively inexpensive, easy to synthesize, thermally stable, have excellent antigen loading capacity[4–6], and most importantly, they can be easily used in the pharmaceutical industry due to their smaller particle size and ability to penetrate lymph nodes and other vital organs to ensure successful drug delivery[6,7].

The use of alumina nanoparticles as potential vehicles for drug and vaccine delivery is generating both excitement and concern among researchers about the safety of such materials under both in vitro and in vivo

[1]Department of Pathology and Microbiology, Faculty of Veterinary Medicine, Universiti Putra Malaysia, 43400 Serdang, Selangor, Malaysia. [2]Department of Science Laboratory Technology, Ramat Polytechnic Maiduguri, Maiduguri 1070, Borno State, Nigeria. [3]Department of Veterinary Clinical Studies, Faculty of Veterinary Medicine, Universiti Putra Malaysia, 43400 Serdang, Selangor, Malaysia. [4]Biophysics Laboratory, Department of Physics, Faculty of Science, Universiti Putra Malaysia, 43400 Serdang, Selangor, Malaysia. [5]Nanomaterial Synthesis and Characterization Laboratory, Institute of Nanoscience and Nanotechnology, Universiti Putra Malaysia, 43400 Serdang, Malaysia. [6]UPM-MAKNA Cancer Research Laboratory, Institute of Bioscience, Universiti Putra Malaysia, 43400 Serdang, Selangor, Malaysia. ✉email: alhmodubuk@gmail.com; azmi@upm.edu.my

conditions[1,8]. Interestingly, many types of NP such as alumina nanoparticles (AlNP), gold nanoparticles (AuNP), zinc oxide (ZnO), and silica nanoparticles (SNP) have already been studied in various cell lines for drug delivery. However, there are serious concerns about the potential cytotoxicity of such nanoparticles to living cells. It is well documented that nanoparticles with smaller size (5–10 nm) have greater cytotoxicity than larger ones (10–100 nm)[8,9]. In addition, rod-shaped nanoparticles showed higher cytotoxicity compared to round nanoparticles due to recognition by the host immune system[10–12].

It is well known that knowledge in the field of nanomaterials has led to the development of nanoparticles by various techniques, including chemical reduction, sol–gel, laser ablation, sonochemistry, coprecipitation, inert gas condensation, ion sputter scattering, microemulsion, spark discharge[3,4], and template synthesis methods[13–15]. However, these techniques have been reported to have serious toxic effects both in vitro and in preclinical animal systems[10]. Therefore, the hazardous cytotoxic chemicals[9,16] and time-consuming multi-step cultivation of microorganisms[17,18] need to be replaced by inexpensive and safe green chemistry methods for nanoparticle synthesis[18,19].

Inorganic nanomaterials such as AlNPs synthesized using plants have attracted much attention due to their remarkable physicochemical and phytochemical properties with remarkable biochemical benefits[12,14,20–22]. The potential phytochemical parameters such as alkaloids, tannins, saponins, tannins, polyphenols[17] and steroids can be easily involved in the stabilization and reduction of aluminum nitrates to alumina nanoparticles[20,23]. Alumina nanoparticles are remarkable inorganic nanoparticles that have diverse biological applications such as vaccine adjuvants[24,25], drug delivery, and wastewater treatment[3] due to their biological and mechanical properties[17,26–28].

Alumina (Al_2O_3) nanoparticles are a type of nanomaterials with enormous medical applications. Aluminum (Al) is the third most abundant metallic element after silicon and oxygen[29]. It is a light, dense, silvery metal extracted from bauxite in the earth's crust[9]. It is used in many medical, industrial and environmental applications[23,30]. Nanoparticles of elemental alumina exhibit remarkably good biological and physiochemical properties[23], such as biocompatibility, low toxicity, improved optical properties, easy surface functionalization, and antimicrobial properties[11,31]. Aluminum salts and hydroxides are known for their excellent interactions with peptides and proteins in host cells. There may be a strong evolutionary pressure to find amino acid residues for incorporation into peptides[32] and proteins that reduce potential precipitation and self-aggregation in solution[22]. This property has led to beneficial applications of aluminum nanoparticles in medicine and environmental applications such as water purification[3].

In addition to peptides and protein interactions in biological systems, aluminum exquisitely aggregates numerous other classes of biomolecules, such as blood coagulation glycoproteins, cytostructural neurofilaments, amyloid and non-amyloid peptides, phospho-protein in milk, and especially amyloid plaque nuclei, which play an essential role in immunopathological and pro-inflammatory consequences[11,23]. Interestingly, among all biologically known divalent and trivalent metallic transition elements, aluminum has been reported to exhibit remarkable biocompatibility with DNA from plants and animals[8].

However, there are serious concerns about the potential toxicity and incompatibility of such alumina nanoparticles in living systems[33]. Therefore, rapidly and environmentally friendly synthesized alumina nanoparticles serve as an alternative to conventional chemical synthesis and have attracted much attention due to their remarkable biocompatibility with tissues[34]. Unfortunately, knowledge about the safety and potential toxicity of green synthesized nanoparticles in various mammalian cell lines and experimental animals is still insufficient. Moreover, there is no sound knowledge about the potential uptake and adverse effects of alumina nanoparticles[35]. Therefore, the present study aims to evaluate the in vitro cytotoxicity of AlNPs synthesized using green chemistry approaches[36]. To evaluate the biological safety and potential toxicity, we used Vero and LT cells and studied the nanoparticles at different concentrations. The results of this work are supported by optical microscopy, electron microscopy and fluorescence microscopy.

Materials and methods

The reagents used are of analytical grade and the chemicals were used without additional treatment. Aluminum nitrate (99.98%), methanol (99.8%), anhydrous DMSO (dimethyl sulfoxide), and MTT powder. The cell lines (VERO and LT) were provided by our group with some modifications. The cell lines were originally manufactured by ATCC (catalog number ATCC® CCL-81™) and stored in the virology laboratory.

Collection, identification, and storage of the *Carica papaya* leaves

The samples of fresh leaves of *Carica papaya* were collected under the medicinal plant permit at Universiti Putra Malaysia (UPM) in accordance with applicable institutional, national and international procedures and legislation. The plant was identified at the Biophysics Research Laboratory (BRL) of the Faculty of Science, UPM by Associate Prof. Azurahanim C., confirming the kingdom, family and species. To support reproducibility, plant voucher specimens were deposited in the BRL Herbarium, UPM. Fresh, healthy and well-grown leaves of the leaves were collected from Agrobio Farm, UPM, Putrajaya, Malaysia and transported to BRL. The leaves were washed thoroughly with 2 L of deionized water and air dried at room temperature. The leaves were mixed and stored in a 50 mL plastic tube and kept at room temperature for further use.

Green synthesis and purification of AlNPs

As shown in Scheme 1, the synthesis and purification of AlNPs using *C. papaya* leaves as reducing and capping agents was carried out in two steps. AlNPs were synthesized according to a method described by[17] with few changes and optimizations[17]. The synthesis of the NPs was carried out using different concentrations of aluminum nitrate mixed with several volumes of papaya leaf extracts as reducing and capping agents. Briefly, 45 mL, 40 mL, and 35 mL of a 5 mM aluminum nitrate ($Al(NO_3)_3$) solution were added dropwise to 5 mL, 10 mL, and 15 mL

2
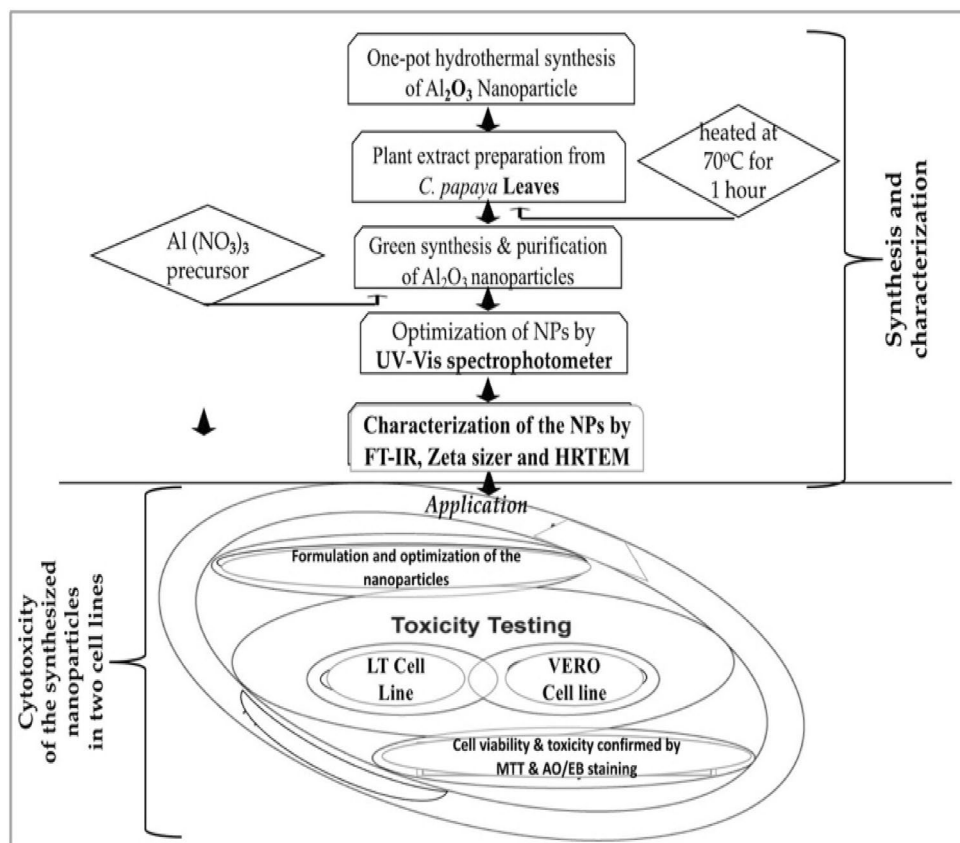
Scheme 1. Schematic diagram of the experimental flowchart: methods for synthetic preparation, characterization, and in vitro evaluation of cytotoxicity of alumina nanoparticles in cell lines (LT and VERO). The experimental framework was carried out in two stages. First, the green synthesis and characterization of the nanoparticles were performed. Then, the potential toxicity was evaluated by cell viability and apoptosis, which were confirmed by MTT assay and AO /EB staining technique.

of the leaf extract solutions, respectively, and heated and stirred gently at 1290 rpm for 25 min until a yellowish, deep brown precipitate was formed, indicating the formation of alumina nanoparticles. The reaction mixture was cooled, and the precipitate was spun at 6000 rpm for 25 min. The pellets were rinsed with double autoclaved water and centrifuged at the same speed. The pellets were cleaned with methanol and double distilled water. Finally, the dried product was calcined at 600 °C for 2 h in a sintering furnace. The AlNPs formed were then ground into fine powder using a pestle and mortar, which was stored in a sterile bottle in a desiccator before further characterization and cytotoxicity studies.

Size, shape and chemical composition of AlNPs

Preliminary confirmation of the synthesized nano-alumina was determined by ultraviolet–visible (UV–Vis) spectral analysis (not showed). The measurement was performed in the wavelength range from 300 to 700 nm using an evolution 220 spectrophotometer. The average particle size distribution and surface charges of the NPs were measured using a DLS instrument. FTIR, and HR-TEM. The spherical HR-TEM structures of the particles were obtained after calcination at 500 °C for 3 h. The dried alumina powder was dissolved in distilled water at a concentration of 2 mg/mL and then sonicated for 15 min to reduce the risk of agglomeration. At the end of the 15-min sonication, a drop of the NPs suspension was placed on a carbon coated copper grid for HRTEM particle size analysis. Then the films were air dried on the grids at temperature. The HR-TEM images were acquired using a JEOL electron microscope[9].

Cell lines, cell culture and cell seeding

The Vero and Lamb testis cell lines and cell culture conditions were kindly provided by Prof. Dato' Dr. Mohd Lila Mohd Azmi, Department of Pathology and Microbiology, Universiti Putra Malaysia, and were obtained from a cryopreserved strain originally produced by ATCC (catalogue number ATCC®, CCL-81™) and stored in the Virology Laboratory. The cell lines were prepared following previous studies by Radziun et al.[13], but with some modifications. Briefly, the frozen Vero cell line was carefully removed from a tank of liquid nitrogen and thawed by immersing the tube containing the cells in a water bath at 37 °C for 2 min to revive the cells. Cells were grown in T_{25} tissue culture flasks containing DMEM medium with 2% (v/v) phosphate-buffered saline, and cells were

allowed to confluence ~ 80 to 90%. The monolayer cell lines were detached from the flasks and the cell number was adjusted to 2.0×10^5 cells/mL with DMEM supplemented with 10% FBS.

Samples preparation, assays for cell viability and proliferation

Prior to cell treatment, nanoparticles were dispersed in FBS-free Dulbecco's Modified Eagle Medium at a stock concentration of 2 mg/mL. Further dispersion of the particles was facilitated by 15 min of sonication (Hielscher Ultrasonics, Germany). The stock solution was further diluted with DMEM to produce different working concentrations. The conventional MTT reduction assay was performed to investigate the cell viability and cytotoxicity of the synthesized AlNPs. The Vero and lamb testis cell lines were grown in 96-well apartment-bottomed plates at a cell density of approximately 2.0×10^5 cells/mL and incubated at 37 °C for 24 h before treatment with the nanoparticles. The cell viability study was performed according to the method of Radziun et al. (2011) with some modifications[2,13]. In brief, both cell lines were exposed to different concentrations of the NPs (0, 10, 60, 120, 240, and 480 μg/mL AlNPs) and incubated for 24 and 48 h. For the cytotoxicity assay, an independent experiment used five replicate wells for the different assay concentrations per plate and a control group containing only the DMEM culture medium without nanoparticles.

The plates were monitored for cell shrinkage and swelling at regular intervals. At the end of each period, cell viability was tested using 5 mg/mL dissolved MTT reagent per well. Plates were gently shaken and cells were allowed to react with MTT for 4 h. At the end of the four-hour incubation period, 85 μL DMEM was carefully removed from the wells, replaced with 100 μL solvent (dimethyl sulfoxide), and gently mixed. The plates were then gently shaken and incubated in a dark box for 30 s to dissolve the formed formazan. Optical density was then measured at A_{590} nm with A_{645} nm as a reference value using a microplate reader (Sun Rise, TECAN, Inc., Baldwin Park, CA, USA). Three independent runs were performed for the cytotoxicity assay[33]. The percentage of viable cells and cytotoxicity were calculated using the following formulas: Percentage (%) of viable cells = (A_{492} in treated sample/A_{492} in control sample) × 100. On the other hand, percentage cytotoxicity was calculated using the following formula: % cytotoxicity = 100 – % cell viability[1,22]. The IC_{50} was determined using the nonlinear regression curve.

Determination of cell viability using double AO/EB fluorescence staining

Double AO /EB (acridine orange/ethidium bromide) fluorescence staining has been used to assess the necrotic nuclei or apoptotic effects of nanoparticles. This technique allows green-stained live cells to be distinguished from red-stained non-viable cells under the fluorescence microscope. Vero and LT cell lines were trypsinized after reaching the logarithmic growth phase with 0.25% trypsin and healthy cells were counted as described by Liu et al. (2015). To perform this assay, a cell density of 2.0×10^5 cells/mL of healthy cells was carefully grown in flat-bottomed 96-well plates (100 μL/well). Then the cells were treated with 0, 10, 60, 120, 240, and 480 μg/mL nano-alumina and incubated for 4 h. The cell lines were also treated with dual fluorescent dyes AO /EB. Cell lines were trypsinized and rediluted on ice with PBS, and the dual AO /EB dyes were mixed gently at a 1:1 ratio (100 μg/mL of each AO /EB dye). 10 μL of the mixture of each cell suspension was carefully dropped onto a fat-free slide and covered with a coverslip. Samples were observed and viable cells were determined under a fluorescence microscope at 40× magnification.

Statistical analysis

Experimental procedures were performed in triplicate. The MTT assay was repeated at least three times. The other two assays (to assess cell viability and apoptosis) were also repeated at least four times. All generated data were expressed as mean ± standard error. FTIR graphs were generated using Origin version 8. Data were analyzed using GraphPad Prism version 9.0 software.

Results

Characterization of alumina nanoparticles

In the study, an extract of *C. papaya* leaves was used as a starting material for the rapid synthesis of the NPs. The yellowish-brown precipitates formed after 10–15 min of mixing the plant extract and the aluminum nitrate solution indicate the formation of aluminum nano-powder. Figure 1 A shows a step in the green synthesis of alumina nanopowder. The observed of color changes from dark brown to yellow precipitate after mixing the aluminum nitrate with the papaya leaf extract was a clear indicative the formation of alumina NPs in the aqueous extract of *C. papaya*. The ZP result shows the colloidal state of the nanoparticles at a value of – 75 mV.

Fourier transform infrared spectroscopy (FT-IR) Analysis
The important biomolecules and infusions acting as reducing and capping agents of the nano-alumina were determined by FTIR. The result showed numerous peaks in the diagnostic and fingerprint regions of the FTIR spectra. The presence of a broad, strong peak at 3200 (O–H stretching), 2200 (C≡C stretching), 1620 (C=N), and 1250 cm^{-1} (C–O stretching) organic functional groups indicates the presence of reducing and capping agents in the plant[37]. However, at 1020, 820, and 581 cm^{-1}, different stretching was observed indicating the presence of alumina (Fig. 1). Thus, the FTIR results showed an effective interaction between OH and the C=O functional groups present in the samples. Therefore, such interactions most likely lead to biocompatibility and environmental friendliness of the synthesized nano-powder[9]. Instead of the individual peaks, a relatively large peak was observed at 3200 cm^{-1}, which could be due to the presence of an organic reducing molecule released from the *Carica papaya* leaf extract and bound to the alumina ion.
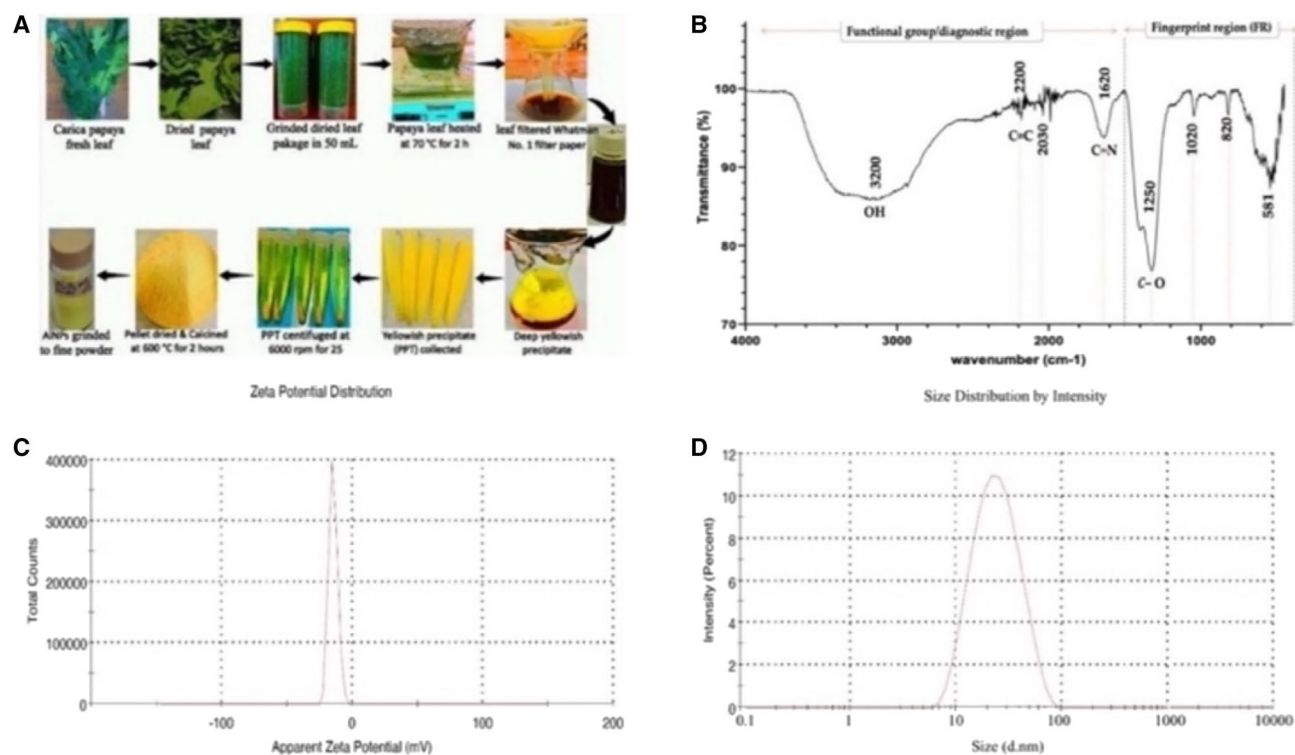
Figure 1. (**A**) schematic representation of the different steps in the synthesis of alumina nanopowder using *C. papaya* extract as reducing and capping agent for precausor aluminum nitrate salt. (**B**), FT-IR spectra of the NPs, (**C,D**) show plots of zeta potential and size distribution of nanoparticles.

Particle size (PA) analysis

Characterization of PA and surface charges (zeta potential) was evaluated DLS and revealed an average hydro-dynamic mean diameter of 52 nm and a ZP value of − 25 to 5 mV in a liquid suspension. This size distribution of intensity (particle size) and ZP surface charge are within the range determined by HRTEM. Figure 1 C and D show the negative surface charge and particle size analysis of plant-assisted synthesis of AlNPs; the average size (47 nm). We further confirmed the particle size determined by DLS using SEM and HRTEM. The images from TEM tend to show larger particle size compared to HRTEM. As shown in Fig. 2, the particles in the images from SEM (Fig. 2c & d) had a slightly larger diameter than those measured by HRTEM (Fig. 2a,b). Smaller NPs had an average size of 25 and 36 nm with HRTEM and SEM, respectively. For larger particles, the average size was 50 and 61 nm, respectively. However, some agglomerations were clearly visible on the HR-TEM image, which could be due to the addition of some drops of the nanoparticles on the microgrid during sample preparation. Moreover, the variations in particle size observed in the HR-TEM images could be due to the different crystal compartments aggregated in the particles.

MTT assay as a cytotoxic study in VERO cell lines

The Vero cell lines were exposed with of alumina nanoparticles for 24 and 48 h. Then, the IC_{50} values were obtained from the cytotoxicity curve. The potential toxicity of the nanoparticles on the mammalian cell lines was determined by both microscopic and colorimetric analyzes using the MTT assay in triplicate[33]. The possible significant differences between cell lines treated with NPs compared with untreated Vero cell and estimated by one-way analysis ANOVA. The living healthy cells synthesized deep purple colored crystal formazan, indicating a potential cytotoxic effect of the nanoparticles, which consequently reduced the number of viable cells and thus decreased in color intensity. The percentage of cell death was estimated by comparing crystal formazan synthesis in exposed cell lines with formazan synthesis in unexposed cell lines (control). The cytotoxicity of the untreated Vero cell lines (Fig. 3a) adhered completely to the surface of the plate, were confluent, and showed no cell shrink-age or apoptotic cell bodies when viewed under the microscope. However, the cell lines Vero, exposed to different concentrations of the NPs for 24 and 48 h (Fig. 3c,d) and (Fig. 4c,d), respectively, showed a slight and significant decrease in cell viability once the concentration increased to 480 μg/mL, with a significant decrease in the syn-thesis of crystal formazan (Fig. 5g), reaching low formazan production (Fig. 5g) at 480 μg/mL. Interestingly, the repeated triplicate results did not show significant differences between the assays performed, as determined by the one-way method ANOVA. On the contrary, the cell lines exposed to the concentration < 60 μg/mL (Fig. 3 and 4b,f) showed no significant change in formazan synthesis, indicating no cytotoxicity, as the number of live cells remained barely intact.
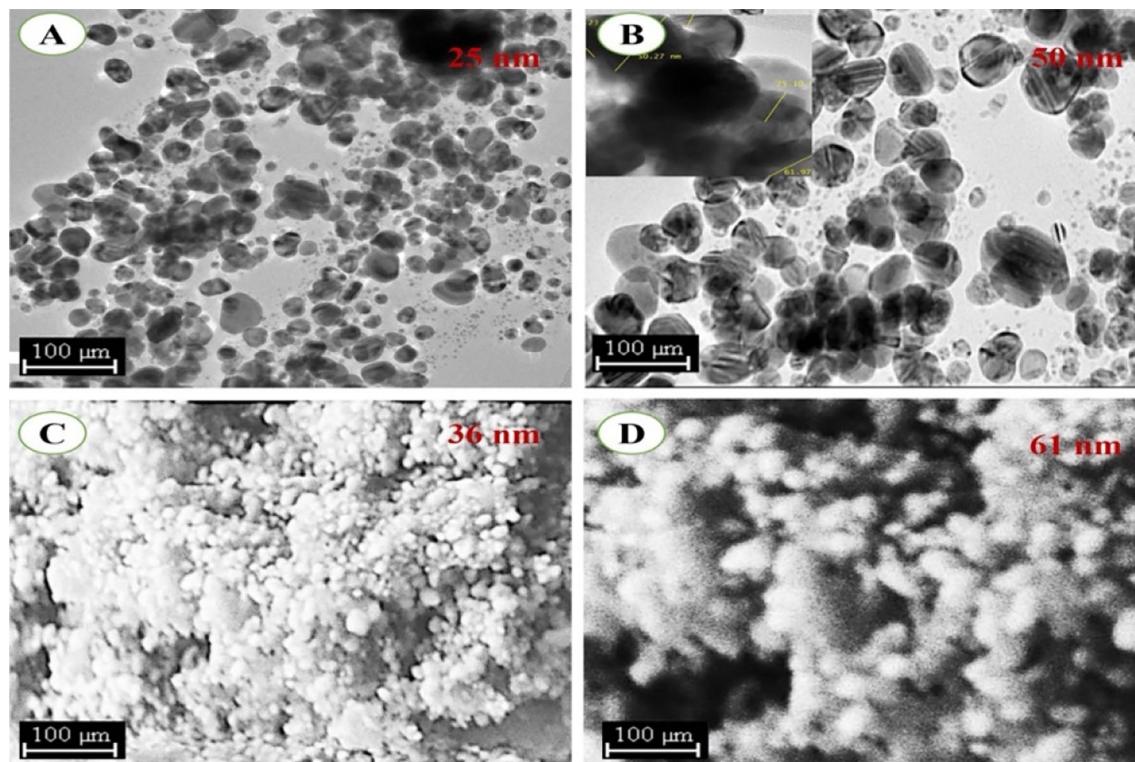
Figure 2. HRTEM (upper part; panels **A,B** 25 nm–50 nm) and SEM (lower part; panels **C,D**; 36–63 nm) images of AlNPs nanoparticles with different particle sizes.
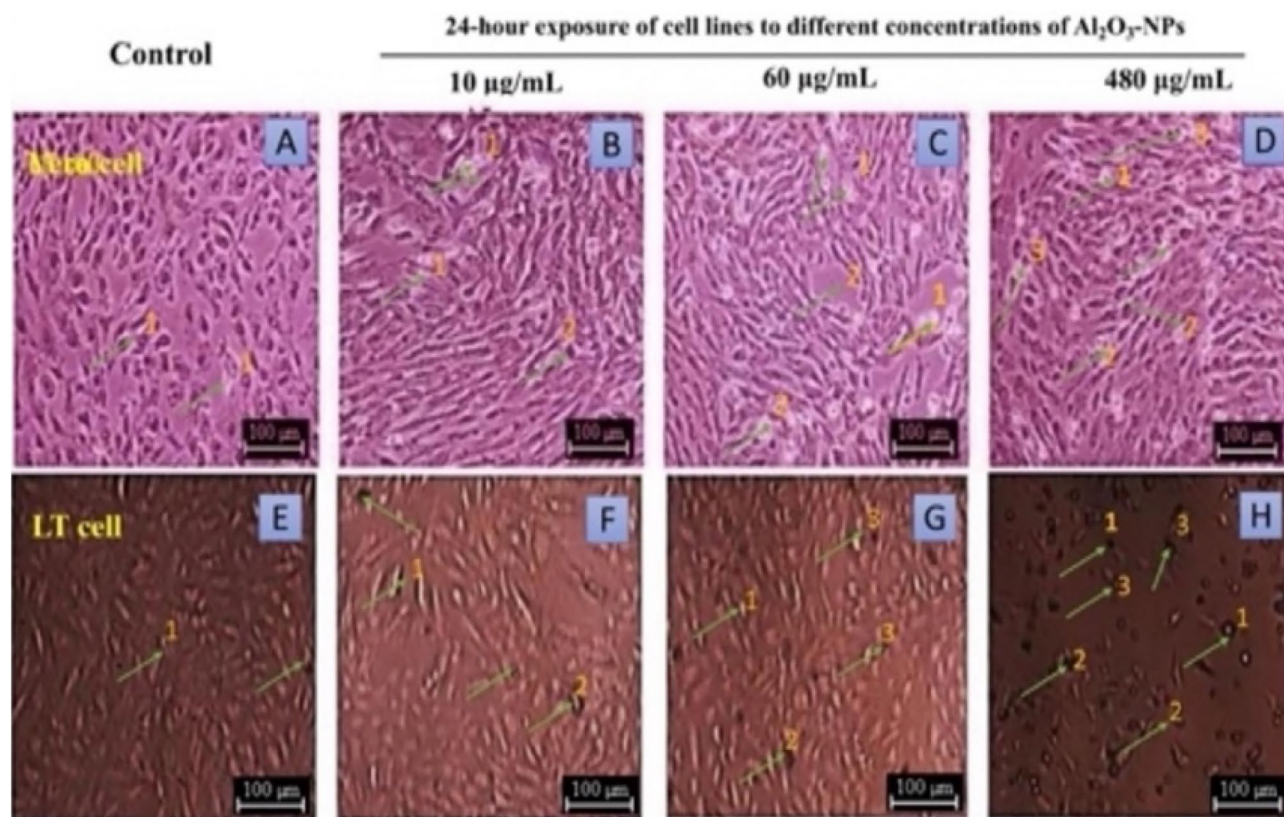

Figure 3. Concentration-dependent toxic effect of AlNPs on cell viability. The images show the morphological changes caused by different concentrations of alumina nanoparticles in selected Vero cell lines under the light microscope. Cells were treated with the nanoparticles for 24 h and imaged under the microscope ($\times$ 40 magnification). The green arrows indicate the shrinkage of the cells.
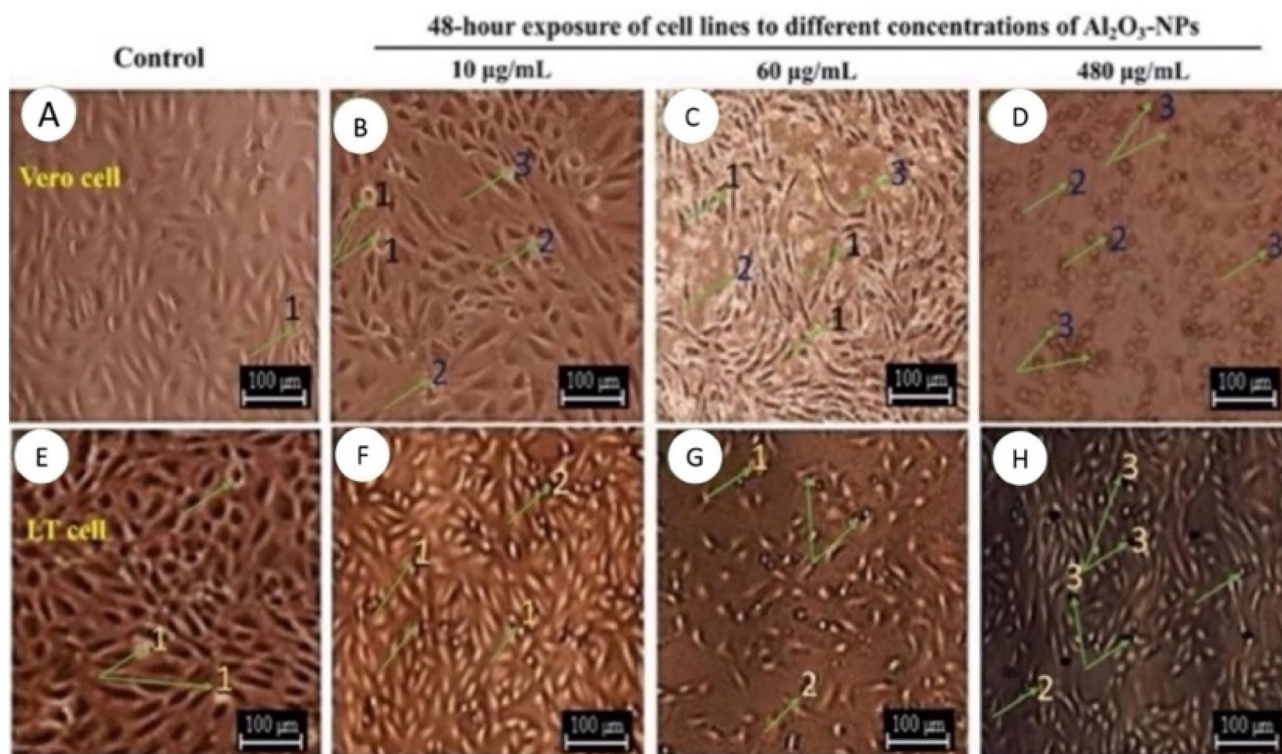
Figure 4. Morphological changes observed upon exposure of LT cell lines treated with different concentrations of alumina nanoparticles. Cells were viewed under a microscope ($\times$ 40 magnification) after 48 h of incubation. The arrows indicate dead cells with normal and apoptotic bodies. The green arrows show increased shrinkage of cells compared to 24-h exposure of both cell lines to different concentrations of nanoparticles.

Cytotoxicity of NPs in LT cell lines

The healthy, adherent, confluent, and oval viable cell morphology of the LT cell lines is reported in Fig. 3 and 4a,e. The MTT assay confirmed the viability of the cells in terms of formazan formation (Fig. 5). LT cell lines with NPs for 24 h (Fig. 3g,h) and 48 h (Fig. 4g,h) showed a slight increase in cell mortality both in terms of cell morphology (cell shrinkage, detached and apoptotic bodies) (Fig. 3 and 4h) and formazan synthesis (Fig. 5 g,h), with slight differences within the assays as indicated by one-way ANOVA.

The cytotoxicity curves from the MTT assays for 24- and 48-h periods for each of the cell lines are shown in Fig. 6a,b. The IC_{50} of the nanoparticles for each of the cell lines was determined by extrapolating the dashed lines from the y-axis to the x-axis as shown in Fig. 6a,b. The IC_{50} of AlNPs in the VERO and LT cell after 24 and 48 h of treatment are recorded as $\sim$ 62, 78 μg/mL and $\sim$ 68, 89 μg/mL, respectively as shown in Fig. 6. Interestingly, the treated cell lines did not show significant toxicity values (mean $\pm$ SEM of three repeated exposures. This confirms the biological safety of the nanoparticle in terms of the absence of significant toxic effects in both cell lines, as shown in Fig. 7c,d.

The NPs were tested on Vero and LT cell lines, which are recommended for evaluating the cytotoxic effect of NPs. Therefore, the cytotoxic effects of different concentrations (10–480 μg/mL) of the newly synthesized alumina nanoparticles were successfully investigated after 24- and 48-h incubation, as shown in Figs. 3, 4 and 5a,b. Evaluation of MTT assays on two mammalian cell lines revealed statistically significant $p < 0.001$ and $p < 0.05$ Fig. 8.

Detection of cytotoxicity in vero and LT cells AO /EB staining assay

In addition, the apoptotic effect of the nanoparticles on two mammalian cell lines was evaluated using AO/EB staining (Fig. 9). Fluorescence micrographs of Vero and LT cell lines treated with a fixed IC_{50} concentration (62 μg/mL) of alumina nanoparticles for 24, 48, and 96 h. The dye AO stains both viable and dead cells green, while EB (ethidium bromide) stains dead cells (apoptotic) orange/red[14]. The AO /EB double staining results also show a few dead cells in the Vero and LT cell lines. Thus, the morphology of normal and apoptotic cells shows a significant number of living cells, as shown in Fig. 9.

Discussion

The recent increase in demand for the application of nanoscale in the field of biomedical sciences has led to the synthesis, characterization, and in vitro safety assessment of nanoparticles. Despite the great successes achieved in nanotoxicological research, the relationship between the in vitro toxicity of nanoparticles and their particle sizes and physicochemical parameters has not yet been clearly established[1,26,32]. In the synthesis of NPs, the choice of a non-hazardous and biocompatible substance is the key strategy to minimize the potential cytotoxic effects of nanoscale in cell lines[2,31]. However, existing data on the cytotoxicity of chemically synthesized nanoscale
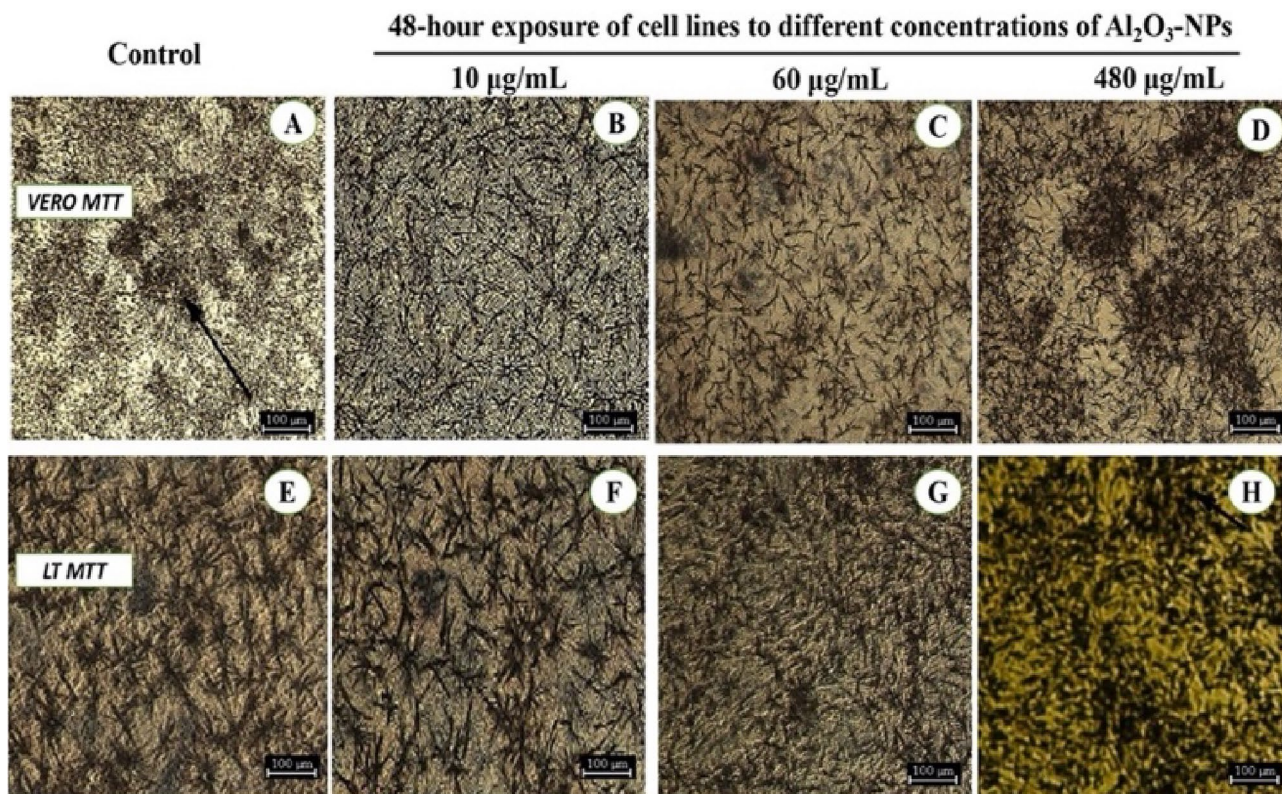
Figure 5. Photomicrographs showing the formation of MTT formazan crystals upon treatment of VERO and LT cell lines with various concentrations of nano-alumina exposed for 48 h. (**A** and **E**) AlNPs with the concentration of 0 μg/mL, (**B** and **F**) AlNPs with the concentration of 10 μg/mL, (**C** and **G**) AlNPs with the concentration of 120 μg/mL, (**D** and **H**) AlNPs with the concentration of 240 μg/mL, × 100. Morphological examination by inverted microscope revealed insoluble formazan crystal formation, which directly correlates with the number of live cells.

alumina on mammalian cell lines are insufficient. Moreover, previous studies reported that the cytotoxic effect of alumina nanoparticles depends on several factors, such as nanoparticle concentration, exposure time, type of cell lines, and nanoparticle size[6,35].

In this study, the synthesized alumina nanoscales were tested on different cell lines to determine biocompatibility for potential biological applications. In vitro toxicity assays using mammalian cell lines are commonly used to determine the effects of exposure to nanomaterials[6,33]. In vitro assessment of cytotoxic effects of nanoparticles using mammalian cell lines is an alternative method for testing cytotoxicity instead of in vivo toxicity using laboratory animal models[2,20,22,38], which are more expensive and difficult to handle compared to in vitro testing[2,6,13,33,35]. Therefore, treatment of cell lines with various concentrations of nanomaterials serves as a preliminary safety or cytotoxic evaluation of the nanoparticle prior to immunization and toxicological studies in preclinical animal models that avoid potential animal death[13]. Therefore, in vitro cell viability studies of nanoscale are an important step in cytotoxic evaluation to assess the potential cellular response to nanoscale based on cell viability, cell death, and metabolic activity[6,30].

Alumina nanoparticles (AlNPs) are known for their toxic effects on mammalian cells. However, previous reports have shown that chemically synthesized nano-alumina is cytotoxic to mammalian cell lines in vitro, leading to a reduction in cell viability[1,33]. The cytotoxic effects of nanoscale largely depend on the physicochemical properties, such as the type of crystallites, surface topography, particle morphology (size, shape, surface area), phase purity, and, most importantly, the concentration of the synthesized particles[37]. Therefore, rapidly and environmentally friendly synthesized nanoparticles serve as an alternative to conventional chemical synthesis and have attracted much attention due to their remarkable biocompatibility with tissues[1,2,20,22,38]. We synthesized AlNPs by a plant-assisted green synthesis method as reported by De et al.[10]. The use of plant extracts has reduces the toxicity of the nanoparticles compared to chemical synthesis, which uses hazardous chemicals as reducing agents[33,39]. The internal and external morphology of the synthesized nanoparticles observed on SEM and HRTEM micrographs showed (Fig. 2a,b) a homogeneous nanoscale structure from 27 to 52 nm with negative surface charge (Fig. 1c,d). Our SEM (52–95 nm) and HRTEM (9–179 nm) particle size results are in agreement with previous AlNPs size results[13,40]. Similarly, our values for average particle size and zeta potential of 52 nm and − 25 to 5 mV, respectively, are in agreement with previous results (− 5 to 5 mV, zeta potential)[2,13,17].

Double fluorescence staining AO /EB is a quantitative, robust method to detect morphological features and changes between normal and apoptotic cells. Acridine orange penetrates untreated (normal) and apoptotic cells with undisrupted membranes[1,13] and fluoresces green after binding to DNA[41]. Ethidium bromide (EB), on the
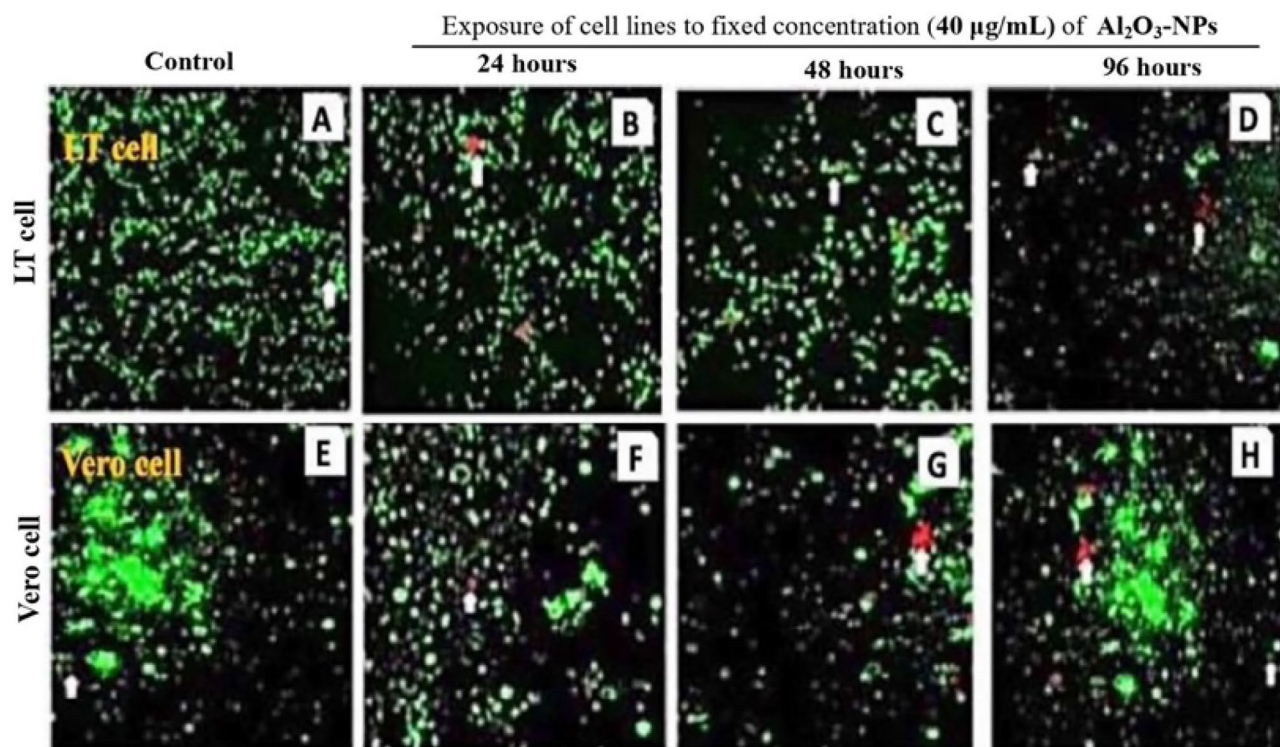
Figure 6. Fluorescence micrographs of Vero and LT cell lines treated with 120 μg/mL alumina nanoparticles and incubated for 48 and 96 h, respectively. The Vero and LT cells were double stained with AO/EB, and images were taken at × 400 magnification. The live cells in the untreated group (normal cells) showed a circular and green nucleus in fluorescence staining (acridine orange staining). In contrast, the apoptotic cells showed granular and orange-red nuclei irregularly distributed on the cell. The white arrow indicates apoptotic cells (red staining).

other hand, can only penetrate cells with disrupted membranes (dead cells), resulting in an orange-red colour when viewed under a fluorescence microscope. In this study, most cells glowed green, indicating that the cells were viable; only a few dead cells appeared red, as shown in Fig. 9.

We found that the cytotoxicity (IC_{50}) of our green alumina nanoparticles appears to be higher than that of Vero cell lines for the cell line LT at the same concentrations and exposure times. Nonlinear regression graph were plotted (Fig. 8a,b) to determine the dose at which 50% of the cells died upon exposure to the NPs. The alumina NPs showed an IC_{50} of 153.3, 186.6 μg/mL in the Vero cell lines for 24 and 48 h of exposure and 252.0, 395.3 μg/mL in the LT cell lines after 24 and 48 h. The IC_{50} results suggest that a lower concentration of nano-alumina is required to achieve 50% mortality[38]. However, the degree of cytotoxicity of nanoscale on mammalian cell lines observed in the present study appears to be generally lower than the higher toxicity reported by Ansari et al.[1,13,38,39] in their study of the cytotoxic effects of chemically synthesized nano-alumina in mammalian cell lines[10,11]. Therefore, the cytotoxic effects of NPs are concentration- and time-dependent, as the results of exposure to alumina nanoparticles in the different mammalian cell lines have been reported in almost all existing studies[10–13,38,39,41].

Interestingly, our results indicate a nearly intact viability of cells when exposed to low concentrations of nanomaterials, and they do not lead to severe cell death as observed with chemically synthesized nanomaterials[10]. These results are consistent with the studies of[10], which reported that incubation of cell lines with nanoparticles showed no cytotoxic effect on Vero and LT cell lines after 24 and 48 h of incubation, as shown in Fig. 7a,b, respectively. It became clear that the cytotoxicity was cell type and concentration dependent, as the cell viability of the Vero cell line gradually decreased with increasing doses from 10 to 480 μg/mL after 24 h of incubation, Fig. 7 c and d. Similar results were observed in the samples with 48 h of exposure time in the two different cell lines[10]. However, the dose-dependent response is enhanced with increasing incubation time, and for the same incubated doses, cell viability was reduced more with longer incubation time. The results are in agreement with those of Ansari et al. who confirmed no significant toxic effect of AlNPs normal cell lines treated with different concentrations of the nanoparticles.

The results of this study clearly showed concentration-dependent cytotoxicity for both the Vero and LT cell lines, whereas the corresponding control group containing only DMEM culture medium without the nanoparticles showed no significant difference at the lower concentrations of nanoparticles from 10 to 240 μg/mL. The result in Fig. 6 shows that the green synthesized alumina NPs caused a slight but significant increase in cytotoxicity against the cell line LT during the 48-h treatment period when the concentration of NPs increased to 240 μg/mL AlNPs ($p < 0.05$). Moreover, cell injury was statistically higher at the highest concentration of 480 μg/
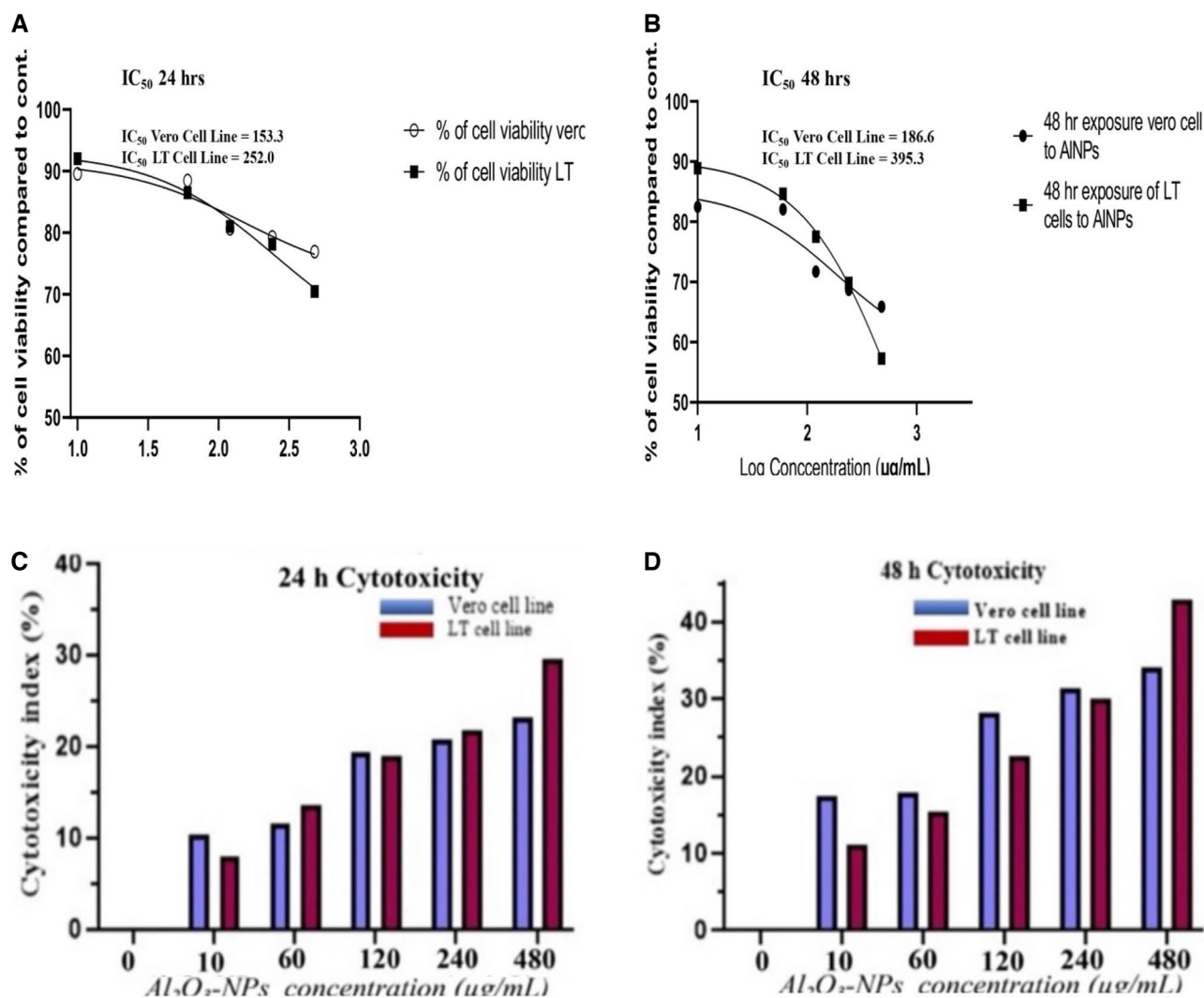
Figure 7. Cytotoxic effect of different concentrations of alumina nanoparticles on Vero and LT cell lines. The potential cytotoxic effect of alumina nanoparticles on VERO and LT cell lines was evaluated as a function of dosage concentration and shown in graphs. The half-maximal inhibitory concentration (IC50) of alumina nanoparticles in the VERO and LT cells at the end of 24- and 48-h incubations was determined using nonlinear regression. The IC_{50} for the two cell lines was 153.3, 252.0 μg/mL and 186.6, 395.3 μg/mL, respectively. Interestingly, the treated cell lines did not show significant toxicity values (mean ± SEM of three repeated exposures).

mL nanoparticles in both cell lines treated with the same concentration of NPs ($p < 0.001$). Interestingly, almost 69% of the cell lines maintained their viability after exposure to the highest concentrations of NPs. In a similar study, the AlNPs were found to have minimal toxicity on normal cell lines, making them preferred candidates for biomedical applications[1,11].

Conclusion

Characterization of the synthesized NPs by HRTEM and zeta potential measurements confirmed that the NPs were negatively charged and spherical agglomerates rather than elongated NPs[13,26]. The negative zeta potential value indicates high susceptibility to tissue absorption and biodistribution[1–3,6]. This is the result of using the natural plant extract as a reducing agent instead of the conventional hazardous chemicals reported in previous studies[1,6,13,23,26]. Our plant-synthesized alumina nanoparticles (AlNPs) have shown reduced cell mortality even at higher concentrations of up to 480 μg/mL for 48 h, with 75% of Vero cell lines still viable. This confirms the biosafety of our recently synthesized nanoparticles in mammalian cell lines compared to chemically synthesized AlNPs, which at approximately the same concentration of nanoparticles (500 μg/mL) yield only 32.20% cell viability in Vero cell lines for only 24 h of exposure time[1]. Therefore, our result suggests that AlNPs at the concentration used in this study have no significant cytotoxic effects (mean ± SEM of three repeated exposures) on the Vero or LT cell lines. Therefore, the green synthesized AlNPs could be used for medical applications such
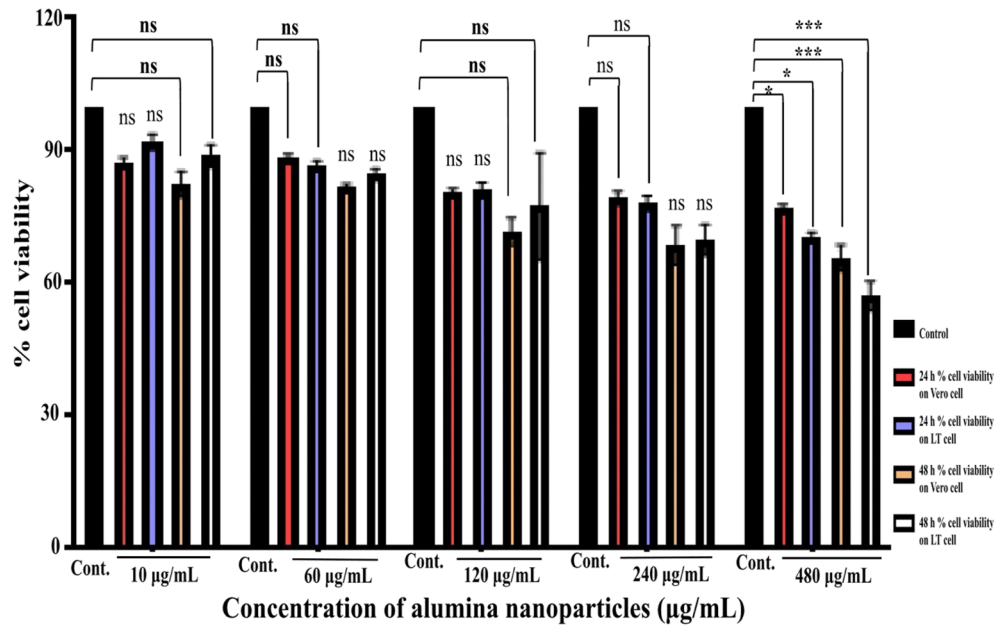
Figure 8. Comparison of 24-h and 48-h cell viability results with the MTT assay. The graph shows the percent cell viability plotted against different concentrations of Al_2O_3-NPs. Healthy mammalian cell lines Vero and LT were exposed to 10, 60, 120, 240 and 480 µg/mL AlNPs and incubated for 24 and 48 h. There is no significance difference between the cell lines exposed to concentrations of nanoparticles ranging from 10 to 240 µg/mL as compared to control groups. However, the results after 48 h of exposure to the highest concentration of nanoparticles (480 µg/mL) clearly show statistically significant values compared to the untreated group when analysed using One Way ANOVA; ***$p < 0.001$ and *$p < 0.05$.
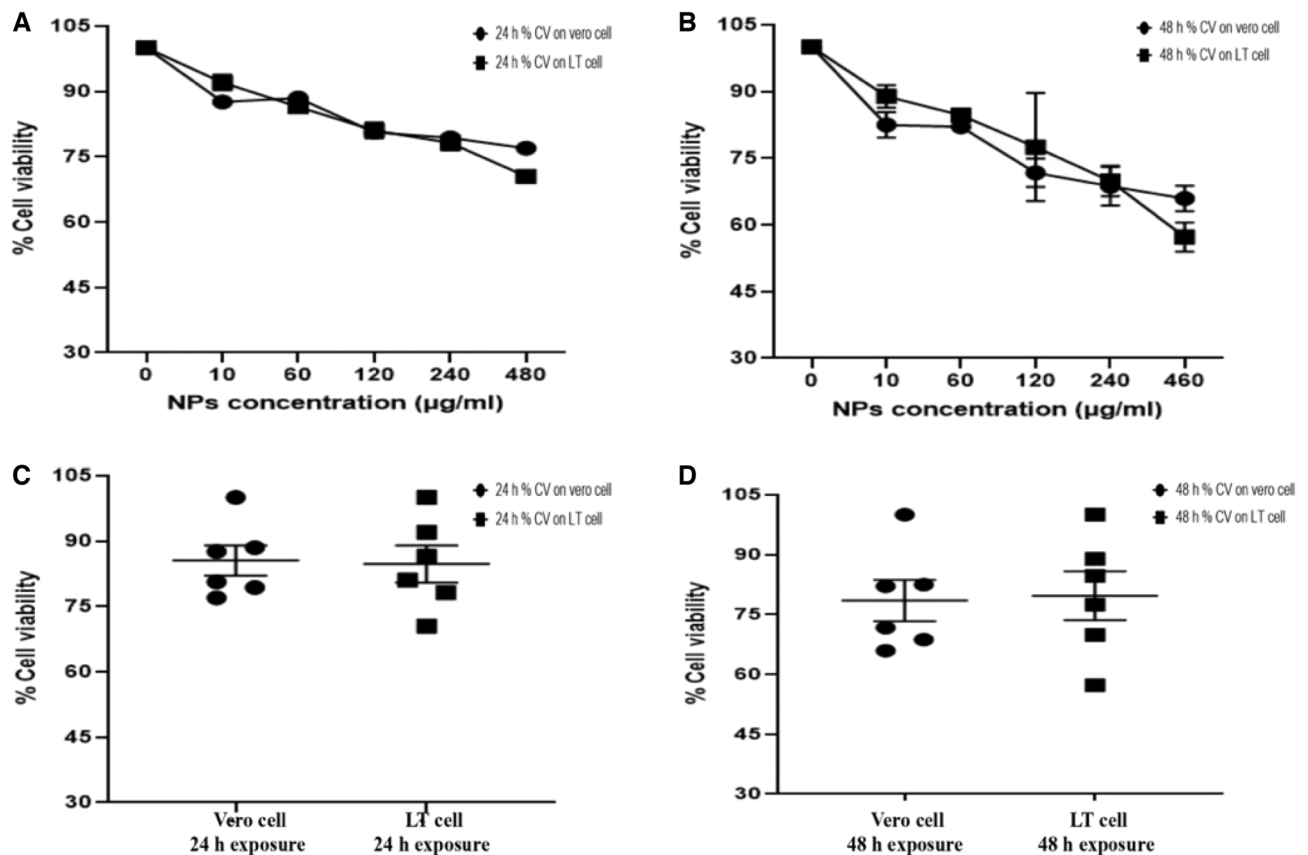

Figure 9. Cell viability of alumina nanoparticles on Vero cell line (**A** and **C**) and LT cell lines (**B** and **D**).

as vaccine and drug delivery. However, further clinical studies in experimental animals are needed to determine the toxicity at the cellular level.

Data availability

The relevant materials and datasets supporting the findings of this original research article are already included in in the main paper, and any other supplemental data generated during the conduct of this research are available upon reasonable request from the corresponding author.

References

1. Arul Prakash, F., Dushendra Babu, G. J., Lavanya, M., Vidhya, K. S. & Devasena, T. Toxicity studies of aluminium oxide nanoparticles in cell lines. *Int. J. Nanotechnol. Appl.* **5**(2), 99–107 (2011).
2. Dong, E. *et al.* Toxicity of nano gamma alumina to neural stem cells. *J. Nanosci. Nanotechnol.* **11**(9), 7848–7856. https://doi.org/10.1166/jnn.2011.4748 (2011).
3. Khan, I., Saeed, K. & Khan, I. Nanoparticles: Properties, applications and toxicities. *Arab. J. Chem.* **12**, 908–931. https://doi.org/10.1016/j.arabjc.2017.05.011 (2019).
4. Wang, N., Qiu, C., Chen, M., Liu, T. & Wang, T. Covering aluminum oxide nanoparticles with biocompatible materials to efficiently deliver subunit vaccines. *Vaccines* **7**, 1–20. https://doi.org/10.3390/vaccines7020052 (2019).
5. Shrivastava, R., Raza, S., Yadav, A., Kushwaha, P. & Flora, S. J. S. Effects of sub-acute exposure to TiO_2, ZnO and Al_2O_3 nanoparticles on oxidative stress and histological changes in mouse liver and Brain. *Drug Chem. Toxicol.* **37**, 336–347. https://doi.org/10.3109/01480545.2013.866134 (2014).
6. Rajiv, S. *et al.* Comparative cytotoxicity and genotoxicity of cobalt (II, III) oxide, iron (III) oxide, silicon dioxide, and aluminum oxide nanoparticles on human lymphocytes in vitro. *Human Exp. Toxicol.* **35**(2), 170–183. https://doi.org/10.1177/0960327115579208 (2016).
7. Gomes, A. C., Mohsen, M. & Bachmann, M. F. Harnessing nanoparticles for immunomodulation and vaccines. *Vaccines* https://doi.org/10.3390/vaccines5010006 (2017).
8. Beyzay, F., Hosseini, A. Z. & Soudi, S. Alpha alumina nanoparticle conjugation to cysteine peptidase A and B: An efficient method for autophagy induction. *Avic. J. Med. Biotechnol.* **9**, 71–81 (2017).
9. Krause, B. *et al.* Characterization of aluminum, aluminum oxide and titanium dioxide nanomaterials using a combination of methods for particle surface and size analysis. *RSC Adv.* **8**, 14377–14388. https://doi.org/10.1039/c8ra00205c (2018).
10. De, A., Chakrabarti, M., Ghosh, I. & Mukherjee, A. Evaluation of genotoxicity and oxidative stress of aluminium oxide nanoparticles and its bulk form in *Allium cepa*. *Nucleus (India)* **59**, 219–225. https://doi.org/10.1007/s13237-016-0179-y (2016).
11. Ansari, M. A. *et al.* Interaction of Al_2O_3 nanoparticles with *Escherichia coli* and their cell envelope biomolecules. *J. Appl. Microbiol.* **116**, 772–783. https://doi.org/10.1111/jam.12423 (2014).
12. Yang, Y. *et al.* Toxicity assessment of nanoparticles in various systems and organs. *Nanotechnol. Rev.* **6**, 279–289. https://doi.org/10.1515/ntrev-2016-0047 (2017).
13. Radziun, E. *et al.* Assessment of the cytotoxicity of aluminium oxide nanoparticles on selected mammalian cells. *Toxicol. Vitro* **25**, 1694–1700. https://doi.org/10.1016/j.tiv.2011.07.010 (2011).
14. Ashajyothi, C., Handral, H. K. & Prabhurajeshwar, C. Applications of metal and metal oxide-based nanomaterials in medical and biological activities. In *Handbook of Research on Green Synthesis and Applications of Nanomaterials* (eds Garg, R. *et al.*) 312–337 (IGI Global, 2021).
15. Tanna, J. A., Chaudhary, R. G., Gandhare, N. V. & Juneja, H. D. Alumina nanoparticles: A new and reusable catalyst for synthesis of dihydropyrimidinones derivatives. *Adv. Mater. Lett.* **7**, 933–938. https://doi.org/10.5185/amlett.2016.6245 (2016).
16. Lekeufack, D. D. & Brioude, A. One pot biosynthesis of gold NPs using red cabbage extracts. *Dalton Trans.* **41**, 1461–1464. https://doi.org/10.1039/c2dt11839d (2012).
17. Ansari, M. A. *et al.* Green synthesis of Al_2O_3 nanoparticles and their bactericidal potential against clinical isolates of multi-drug resistant *Pseudomonas aeruginosa*. *World J. Microbiol. Biotechnol.* **31**, 153–164. https://doi.org/10.1007/s11274-014-1757-2 (2015).
18. Iqbal, J. *et al.* Green synthesis and characterizations of nickel oxide nanoparticles using leaf extract of *Rhamnus virgata* and their potential biological applications. *Appl. Organomet. Chem.* **33**, 1–16. https://doi.org/10.1002/aoc.4950 (2019).
19. Piriyawong, V., Thongpool, V., Asanithi, P. & Limsuwan, P. Preparation and characterization of alumina nanoparticles in deionized water using laser ablation technique. *J. Nanomater.* https://doi.org/10.1155/2012/819403 (2012).
20. Ghotekar, S. Plant extract mediated biosynthesis of Al_2O_3 nanoparticles-a review on plant parts involved. *Characterization Appl. Nanochem. Res.* **4**, 163–169. https://doi.org/10.22036/ncr.2019.02.008 (2019).
21. Bukar, A. M. *et al.* Evaluation of phytochemical and potential antibacterial activity of *Ziziphus spina-christi* L. against some medically important pathogenic Bacteria Obtained from University of Maiduguri Teaching Hospital, Maiduguri, Borno State—Nigeria. *J. Pharmacognosy Phytochem. JPP* **3**, 98–101 (2015).
22. Kermani, Z. R. *et al.* Aluminium oxide nanoparticles induce structural changes in tau and cytotoxicity of the neuroblastoma cell line. *Int. J. Biol. Macromol.* **120**, 1140–1148. https://doi.org/10.1016/j.ijbiomac.2018.08.182 (2018).
23. Hassanpour, P. *et al.* Biomedical applications of aluminium oxide nanoparticles. *Micro Nano Lett.* **13**, 1227–1231. https://doi.org/10.1049/mnl.2018.5070 (2018).
24. Bukar, A. M. *et al.* Immunomodulatory strategies for parapoxvirus: Current status and future approaches for the development of vaccines against orf virus infection. *Vaccines* **9**, 1–24. https://doi.org/10.3390/vaccines9111341 (2021).
25. Wang, N., Wei, C., Zhang, Z., Liu, T. & Wang, T. Aluminum nanoparticles acting as a pulmonary vaccine adjuvant-delivery system (VADS) able to safely elicit robust systemic and mucosal immunity. *J. Inorg. Organomet. Polym. Mater.* **30**, 4203–4217. https://doi.org/10.1007/s10904-020-01572-z (2020).
26. Subramaniam, V. D., Murugesan, R. & Pathak, S. Assessment of the cytotoxicity of cerium, tin, aluminum, and zinc oxide nanoparticles on human cells. *J. Nanoparticle Res.* https://doi.org/10.1007/s11051-020-05102-3 (2020).
27. Manikandan, V. *et al.* Green synthesis of PH-responsive Al_2O_3 nanoparticles: Application to rapid removal of nitrate ions with enhanced antibacterial activity. *J. Photochem. Photobiol. A Chem.* **371**, 205–215. https://doi.org/10.1016/j.jphotochem.2018.11.009 (2019).
28. Koopi, H. & Buazar, F. A novel one-pot biosynthesis of pure alpha aluminum oxide nanoparticles using the macroalgae *Sargassum ilicifolium*: A green marine approach. *Ceram. Int.* **44**, 8940–8945. https://doi.org/10.1016/j.ceramint.2018.02.091 (2018).
29. Krause, B. C. *et al.* Aluminum and aluminum oxide nanomaterials uptake after oral exposure-a comparative study. *Sci. Rep.* **10**, 1–11. https://doi.org/10.1038/s41598-020-59710-z (2020).

30. Sathiya Narayanan, N., Baskar, N., Vedha Hari, B. N., Sankaran, R. & Ramya Devi, D. Performance of cutting tool with cross-chevron surface texture filled with green synthesized aluminium oxide nanoparticles. *Sci. Rep.* **9**, 1–10. https://doi.org/10.1038/s41598-019-54346-0 (2019).
31. Manyasree, D., Kiranmayi, P. & Ravi Kumar, S. N. Synthesis, characterization and antibacterial activity of aluminium oxide nanoparticles. *Int. J. Pharm. Pharm. Sci.* **10**, 32. https://doi.org/10.22159/ijpps.2018v10i1.20636 (2018).
32. Emetere, M. E. & Ahiara, I. M. Synthesis and characterization of aluminum coated *Carica papaya* extracts. *Chem. Data Collect.* **28**, 100381. https://doi.org/10.1016/j.cdc.2020.100381 (2020).
33. Kumar, V., Sharma, N. & Maitra, S. S. In vitro and in vivo toxicity assessment of nanoparticles. *Int. Nano Lett.* **7**, 243–256. https://doi.org/10.1007/s40089-017-0221-3 (2017).
34. Loh, H. S., Mohd-Lila, M. A., Abdul-Rahman, S. O. & Kiew, L. J. Pathogenesis and vertical transmission of a transplacental rat cytomegalovirus. *Virol. J.* **3**, 1–14. https://doi.org/10.1186/1743-422X-3-42 (2006).
35. Frey, A., Neutra, M. R. & Robey, F. A. Peptomer aluminum oxide nanoparticle conjugates as systemic and mucosal vaccine candidates: Synthesis and characterization of a conjugate derived from the C4 domain of HIV-1(MN) Gp120. *Bioconjugate Chem.* **8**, 424–433. https://doi.org/10.1021/bc970036p (1997).
36. Goutam, S. P., Avinashi, S. K., Yadav, M., Roy, D. & Shastri, R. Green synthesis and characterization of aluminium oxide nanoparticles using leaf extract of rosa. *Adv. Sci. Eng. Med.* **10**, 719–722. https://doi.org/10.1166/asem.2018.2236 (2018).
37. Frey, A. *et al.* Immunization of mice with peptomers covalently coupled to aluminum oxide nanoparticles. *Vaccine* **17**, 3007–3019. https://doi.org/10.1016/S0264-410X(99)00163-2 (1999).
38. Poborilova, Z., Opatrilova, R. & Babula, P. Toxicity of aluminium oxide nanoparticles demonstrated using a BY-2 plant cell suspension culture model. *Environ. Exp. Bot.* **91**, 1–11. https://doi.org/10.1016/j.envexpbot.2013.03.002 (2013).
39. Bukar, A. M. *et al.* Immunomodulatory strategies for parapoxvirus: Current status and future approaches for the development of vaccines against orf virus infection. *Vaccines* **9**, 1341. https://doi.org/10.3390/vaccines9111341 (2021).
40. Doskocz, N., Affek, K., Załęska-Radziwiłł, M. Effects of aluminium oxide nanoparticles on bacterial growth. In *E3S Web of Conferences* **17**, 1–7. https://doi.org/10.1051/e3sconf/20171700019 (2017).
41. Liu, K., Liu, P. C., Liu, R. & Wu, X. Dual AO/EB staining to detect apoptosis in osteosarcoma cells compared with flow cytometry. *Med. Sci. Monit. Basic Res.* **21**, 15–20. https://doi.org/10.12659/MSMBR.893327 (2015).

Author contributions

M.A.M.L., F.F.A.J, C.A.C.A., M.M.N., and A.M.B., were involved in the planning and design of the experiments, A.M.B., C.A.C.A., M.Z.K., and A.N. were involved in the synthesis of the nanoparticles; A.M.B. performed the cell culture experiments M.A.M.-L., F.F.A.J., and M.M.N. contributed reagents; A.M.B., and M.Z.K. analyzed the data; A.M.B. wrote the paper; M.A.M., F.F.A.J., C.A.C.A. and M.M.N. proofread the manuscript. All authors have approved the publication of this article

Funding

Competing interests

The authors declare no competing interests.

Additional information

Correspondence and requests for materials should be addressed to A.M.B. or M.A.M.-L.

Reprints and permissions information is available at www.nature.com/reprints.

Publisher's note Springer Nature remains neutral with regard to jurisdictional claims in published maps and institutional affiliations.